International Journal of Technology (2016) 5: 732-740
ISSN 2086-9614

EFFECTS OF GRADED CONCRETE ON COMPRESSIVE STRENGTHS

Aylie Han[1], Buntara Sthenly Gan[2*], M. Mirza Abdillah Pratama[3]

[1] *Structural and Material Laboratory, Diponegoro University, Semarang 50275, Indonesia*
[2] *Department of Architecture, College of Engineering, Nihon University, Koriyama 963-8642, Japan*
[3] *Department of Civil Engineering, Faculty of Engineering, State University of Malang, Malang 65145, Indonesia*

(Received: March 2016 / Revised: July 2016 / Accepted: July 2016)

ABSTRACT

Concrete is a favoured building material due to its ease of production and use. Even though the concrete mix is designed to have a uniform strength throughout the entire member, casting, as well as the basic characteristics of the concrete materials, could yield a non-homogeneous constitution, resulting in a concrete strength gradation as a function of the depth of the member. A functionally continuous and smooth strength gradation of the concrete member along its axis or section is defined as graded concrete. The objective of this research is to analyse the influence of two different concrete compressive strengths that composed the graded concrete member. The study is split into two parts: the experimental work describing and identifying the mechanical properties of functionally graded concrete and the finite element analysis implementing these property variations in a model. The results showed that the concrete gradation influenced the ultimate strength of a member negatively and altered the stress distribution and displacement response of the specimen.

Keywords: Compressive strength; Concrete; Experimental study; Finite element analysis; Graded concrete

1. INTRODUCTION

Functionally graded material (FGM) is a continuously graded material that has different properties in certain directions within the structure. These properties are the modulus of elasticity, strength, density, and Poisson's ratio (Ramu & Mohanty, 2014). Previous studies have shown that FGM may also increase the residual stress distribution, thermal resistance, and resistance to cracking and reduce the stress intensity factor, so it is a very promising material that requires research for further developments (Birman & Byrd, 2007; Kieback et al., 2003; Chandwani et al., 2015). Although FGM was initially developed using metal materials for spacecraft applications, nowadays it is also studied for building elements such as beams, plates, and shells. Some of these studies used slags substitution (Ashadi et al., 2015) and rice husk ash additive material (Ramadhansyah et al., 2011) in concrete mixtures with the aim of improving the ability of the structure to withstand loads. A research conducted by Dias et al. (2010) showed that the fibres gradually cast on a plate element can improve the production efficiency without reducing the capacity of the structure. The presence of fibres improved the load distribution mechanism and increased the ductility (Mastali et al., 2014; Shin et al., 2007). Most of the studies on concrete FGM used the substitution of materials into the concrete mix to create the gradation in the element. Until now, a research work using a plain concrete mix has

*Corresponding author's email: buntara@arch.ce.nihon-u.ac.jp, Tel./Fax. +81-24-9568735
Permalink/DOI: https://doi.org/10.14716/ijtech.v7i5.3449

not been conducted.

In reality, concrete buildings are designed to have a uniform strength. Imperfections during casting and the characteristics of basic materials could result in a differentiation in concrete compression strength as a function of the depth of a member. Hidayat et al. (2015) conducted a series of non-destructive and destructive tests on a concrete panel having dimensions of 600×600×200 mm, built of plain concrete, with a design strength of 60 MPa. It was confirmed that the bottom part of the test panel had a higher compressive strength when compared to the upper part. The study also included a test case on an existing beam, which again strengthened the presence of gradation in concrete elements.

The study by Hidayat et al. (2015) proved that in reality a concrete member is not uniform and does not possess a homogeneous strength throughout its depth. The main objectives of current study are to find new methods: (1) to create an intentionally graded concrete; (2) to prove methodically that the existing concrete structures are graded. The first objective could lead to optimization regarding material use and production cost. The second objective could lead to optimization regarding the proper assessment of the existing concrete structure conditions and suitable rehabilitation/strengthening methods.

Therefore, the present study is elaborated to produce experimentally and establish a finite element analysis (FEA) tool for graded concrete structures. Therefore, the FEA tool has to be able to verify the experimental results of the graded concrete.

2. EXPERIMENTAL PROGRAMME

2.1. Procedure of Concrete Making and Testing

The procedure of making and testing the graded specimens refers to the study conducted by Gan et al. (2015). Two concrete mixes were assigned: a high strength one having a compressive strength of 60 MPa and a low strength one having a compressive strength of 20 MPa. This considerable difference was chosen to magnify the disparities in concrete properties of the two graded concrete materials. The specimens were further divided into two groups, the uniform cylinders, P60 and P20, and the graded specimens, denoted as G. These graded specimens were cast with the 60 MPa compressive strength at the bottom and the 20 MPa compressive strength in the top layer. Six cylindrical specimens with dimensions of 100×200 mm were prepared for each category and all specimens were tested to a 28-day strength curing time. To eliminate the effect of friction and confinement that occurs between the surface of the specimen and the loading plate, two layers of Teflon, coated with grease were installed in-between the surfaces. The load–displacement responses of the cylinders were further corrected by the response of the Teflon layer.

2.2. Experimental Data

The data were processed statistically to ensure that the responses were correct and represented the actual behaviour of the graded concrete member. The experimental result showed that the uniform concrete specimen P60 reached an average compressive strength of 57.2 MPa with a Poisson's ratio of 0.231; P20 reached an average compressive strength of 24.7 MPa with a Poisson's ratio of 0.266. The average compressive strength obtained from the graded specimen G was calculated as 24.8 MPa. As for Poisson's ratio, the values were a function of the height of the element and were monitored by the use of strain gauges. For this purpose, five pairs of strain gauges were mounted at heights of 25.0, 62.5, 100.0, 137.5, and 175.0 mm, respectively, from the bottom fibres of the cylinder. Based on the former studies, Poisson's ratio and compressive strength gradation as a function of specimen heights were approximated by a linear relationship. These functions were further incorporated into the FEM.

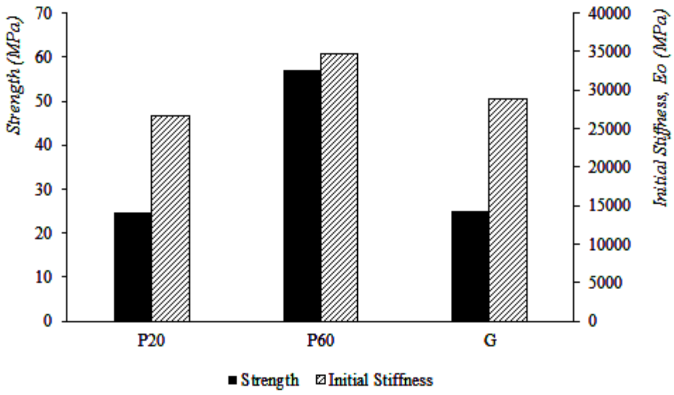

Figure 1 Compressive strength and stiffness modulus of FGC

Figure 1 demonstrates the compressive strength and initial stiffness modulus of the FGC as compared to the P20 and P60 specimens. The FGC specimens had almost an identical strength to the P20 cylinders; the presence of the higher strength concrete had no effect on the overall strength. The initial stiffness of the FGC, however, lay between the stiffness moduli of the P20 and P60 specimens. The P60 and P20 specimens had initial stiffness moduli of 34.69 and 26.61 MPa respectively. The FGC specimen G, which had a stiffness modulus of 28.92 MPa, was thus influenced by the stiffness of both the concrete strengths.

2.3. Visual Observation and Cracking Pattern

Additional specimens were prepared to observe the FGC visually. The cylinders P60, G, and P20, were split along their lengths and were shown in Figure 2.

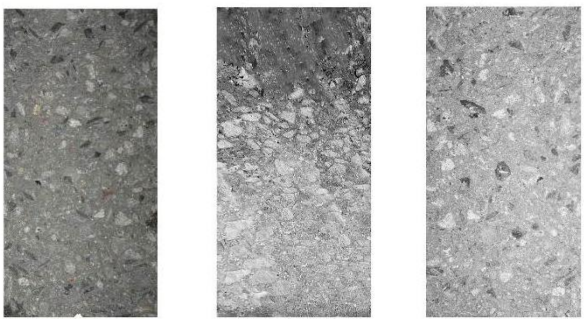

P20 G P60

Figure 2 Visual observation of FGC

The colour grading as well as coarse the aggregate distribution strengthened the conclusion that the production method resulted in a good FGC. P60, which has a substantially higher cement content, appeared to be light-greyish while P20 was dark grey, due to the relatively higher content of coarse aggregates. The G specimen had a dark grey upper layer that gradually turned white.

The FGC specimen G had compressive strength only slightly above that of P20. The crack pattern of the uniform specimens P20 and P60 followed a columnar pattern since the Teflon layer eliminated the confinement from the loading platens. The cracks propagated vertically due to the principal tensile stresses perpendicular to the line of the load. The FGC specimen demonstrated a deviating crack pattern. The cracks started at the weaker concrete strength levels and spread to the cross-section of this layer, as can be seen in Figure 3. This behaviour explained the low compressive strength of the FGC. As soon as the top cross-section of the cylinder failed, the specimen could no longer carry any additional loading.

Figure 3 Crack pattern of FGC versus homogeneous concrete

3. FINITE ELEMENT MODELLING

Strand7 software was used to model the graded concrete specimens and to analyse their behaviour. The output of this finite element analysis (FEA) was validated against the experimental results. Strand7 was chosen as the FEA program because this program accommodates the material's non-linear analysis through the adjustment of parameters. Also, the failure criteria could be modified to approach the conditions and material behaviour of the experimental model as closely as possible.

3.1. Modelling

In this study, the model was analysed as an axisymmetric model. The model was considered to be isotropic, having an identical modulus of elasticity response in all strain directions, even beyond the cracking of concrete. The stress–strain relationship in uniaxial compression and tension is adopted from the CEB-FIB 2010 standard. For the input of parameters into the program, the concrete is expected to behave elastically. The program is intended to be able to read the complete stress–strain curve in both compression and tension. In the non-linear elastic stage, Maximum stress was chosen in favour of the other failure criteria for application to the ductile material.

Axisymmetric models are discretized by using a four-nodal quadrilateral element. The size of meshing is determined solely so that the aspect ratio of the meshed element perimeters is close to 1. Higher ratios will result in poor elements and could lead to bad conditions during the FEA. The boundary conditions for the FEM were adapted to the current state of the experimental testing, enabling horizontal node displacements at the bottom of the model (Hutton, 2004). A displacement-controlled increment was used, ensuring that the bottom nodes moved toward the top nodes, as was the case for the experimental testing where the loading plate was positioned beneath the specimen. During testing, the 20 MPa concrete layers of the graded specimen were therefore placed on the bottom in the opposite configuration to the casting configuration.

3.2. Layer-wise Homogenization

Composite materials for specially graded concrete are classified as a heterogeneous material in microstructure due to its constituents: the mortar matrix and coarse aggregates. In modelling, every small layer of graded concrete possesses a difference in material properties. If the graded concrete is modelled as a heterogeneous material in FEA, it will require an extensive running time, originating from the high degrees of freedom (DOF) within the system's model. To overcome this problem, the graded concrete model was idealized as a structure consisting of several very thin layers, assuming homogeneous material properties for each layer (Banks-Sills et al., 2002).

In this study, six axisymmetric models consisting of 2, 4, 8, 16, 32, and 64 layers were analysed to find the number of layers that would give the most efficient outcome in the analysis. The results of displacement and load on various number of layers used in the analyses are depicted in Figure 4.

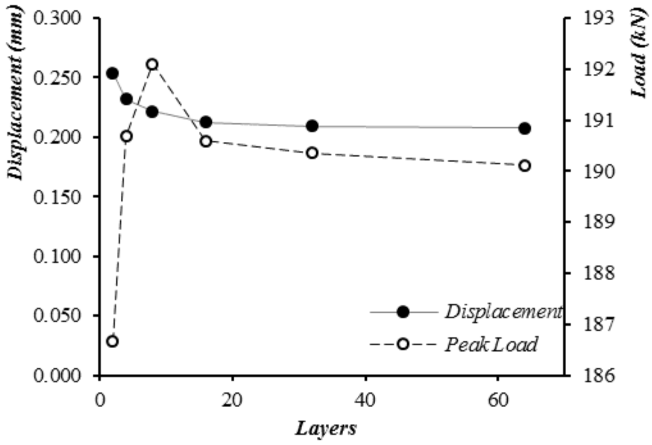

Figure 4 Results of layer number to the displacement and peak load response

The material properties of P60 were set for the top fibres, while the material properties of P20 were set for the outermost bottom fibres. The properties of the material that lie between the two extreme top and bottom fibres were determined based on the linear interpolation approach. The density of concrete for all concrete strengths was considered to be uniform and was set to 2400 kg/m^3. The results of displacement along the concrete specimens of P20, P60 and the graded concrete (G) are shown in Figure 5.

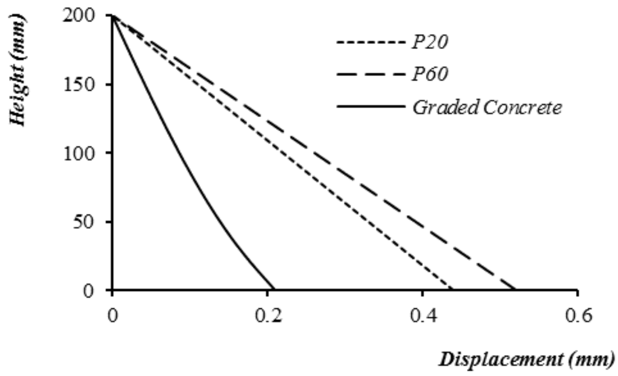

Figure 5 Displacement patterns of P20, P60, and G as a function of layer height

3.3. Iteration Method

The arc-length method is an iterative technique often used in the non-linear analysis since it not only accommodates negative stiffness behaviour, but also can handle snapping and buckling (Crisfield, 1981). The arc-length method uses the predictor and corrector to find the equilibrium path. Use of the appropriate parameters for the predictor and corrector will make the iteration process more efficient. When compared with the Newton-Raphson method, the arc-length method provides a better stability in determining the limit point.

4. RESULTS AND DISCUSSION

4.1. Sensitivity Analysis

The FEA showed that the results became increasingly more convergent as the number of layers of the model increased (Figure 4). The differences in the peak loads and the displacement responses between each succeeding model diminished. The peak load responses increased in the eight-layer models and then showed an almost steady pattern for the models with 16 to 64 layers. Displacement and peak load responses started converging from the 32-layer model to the 64-layer model. With a value of 0.82% for the peak load response and 0.125% for the displacement, the model is considered to be convergent. When the number of layers is increased above 32, the analysis concluded that a non-significant improvement in the obtained data was generated.

4.2. Displacement Pattern

Figure 5 depicts the displacement pattern in the last stage of the FEA for the P20, P60, and G specimens. The data were obtained from the node at the rotational axis of the axisymmetric model. All three curves exhibited a similar pattern; the bottom fibre underwent the largest displacements. The main reason for this behaviour is that, during the experiment, the loading plate was located at the bottom while the upper plate of the apparatus was restrained against vertical displacement.

An interesting fact is that while the displacement response of the uniform members P20 and P60 having the same meshing was linear as a function of the height of the specimen, the graded concrete model G had a polynomial response.

4.3. Results of the Experimental Data and Finite Element Analysis (FEA)

Gan et al. (2015) stated that the peak load achieved by graded concrete having a concrete strength ranging from 20 to 60 MPa was similar to that of the uniform P20, which was equal to 194 kN, in contrast to that of the P60 specimen, which reached 449 kN. The experimental results showed that the compressive strength of graded concrete material was determined by the lowest strength within the specimen. The stress–strain behaviour of P20 and P60 specimens was in good agreement with the CEB–FIB standard. The graded concrete had a stiffness behaviour tending to P60, in combination with a low strength, leaning toward P20. This outcome was in good agreement with experimental data, suggesting that when the ultimate load was reached, the specimen initially failed in the weakest element, followed by failure in the lower perimeter part of the cylindrical specimen. Unlike the graded concrete model, the uniform concrete models tend to have a uniform stress concentration throughout their structure. No stress concentrations were found in the experimental study or FEA. The uniform concrete specimen failed in a columnar crack mode along its height. The FEA by using Strand7 is able to generate the post-peak responses which produced a very close approximation to the experimental results (Table 1 and Figure 6).

Table 1 The results of the experimental data and FEA

Parameter	Experimental	FEM	Sig. (%)
Ultimate Load (kN)			
P20	194.103	194.102	0.0006
P60	449.633	449.497	0.0302
G	194.150	190.352	1.9563
Displacement at Ultimate Load (mm)			
P20	0.396	0.440	11.1575
P60	0.539	0.520	3.5561
G	0.222	0.209	5.5289

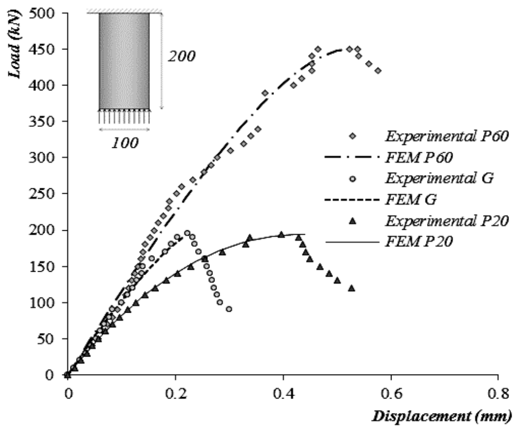

Figure 6 Comparison of load–displacement response between the experimental data and FEA

The reading of the strain gauge mounted on the surface of the graded concrete specimen showed that the strain in the extreme bottom fibre was the largest (Figure 7). This outcome is explained by the fact that for the same load level, a low-quality material having a lower stiffness will experience a larger displacement.

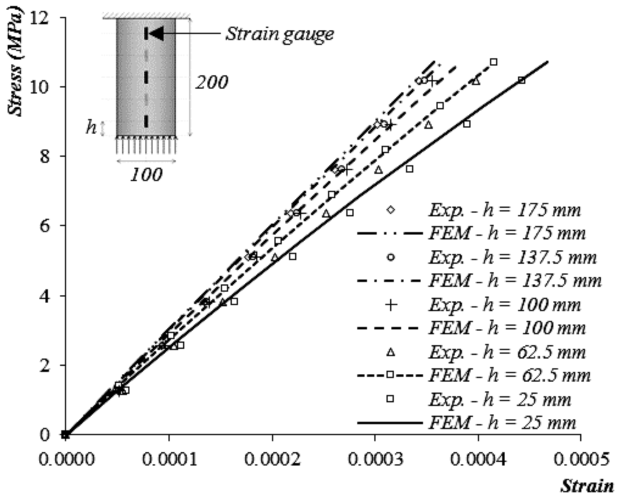

Figure 7 Initial stiffness of graded concrete specimens according to depth

On the top layers, the strain response has a higher gradient, which indicates a higher stiffness when compared to the bottom layer. The stiffness responses of the layers 175 and 137.5 mm from the bottom were very close. This was due to the domination of material failure at the bottom, which disturbed the higher strength material only very slightly at most.

5. CONCLUSION

Visual observation of the colour pattern and aggregate distribution of the split cylinders demonstrated that the method developed was successful in producing a functionally graded concrete material. The accompanying FEM constructed using layer-wise homogenization in combination with an axisymmetric model was proven to be accurate and versatile in predicting the peak load, the load-displacement responses, and the initial stiffness modulus of graded concrete. The number of layers greatly influenced the results. A sensitivity analysis of the number of layers and meshing required to obtain a convergence outcome should be conducted.

It was found that the compressive strength of the graded concrete was influenced by the weaker concrete layers, but regarding stiffness, the graded concrete was affected by both low and high concrete strengths. These findings were confirmed by the FEA. The decreasing of load-carrying capacity of the FGC was due to the initial cracking of the weaker strength concrete layer, creating a crack propagation pattern that deviated from the columnar crack mode observed in the homogeneous specimens. The gradation, however, had little effect on the Poisson's ratio of FGC. As the FEA was proven to be accurate, it can be utilized to analyse a range of concrete FGMs having differences in concrete strengths and multiple concrete strengths in one specimen.

6. REFERENCES

Ashadi, H.W., Aprilando, B.A., Astutiningsih, S., 2015. Effects of Steel Slag Substitution in Geopolymer Concrete on Compressive Strength and Corrosion Rate of Steel Reinforcement in Seawater and an Acid Raid Environment. *International Journal of Technology*, Volume 6(2), pp. 227–235

Birman, V., Byrd, L.W., 2007. Modeling and Analysis of Functionally Graded Materials and Structures. *Applied Mechanics Reviews*, Volume 60(5), pp. 195–216

Chandwani, V., Agrawal, V., Nagar, R., Singh, S., 2015. Modeling Slump of Ready Mix Concrete using Artificial Neural Network. *International Journal of Technology*, Volume 6(2), pp. 207–216

Crisfield, M.A., 1981. A Fast Incremental/Iterative Solution Procedure that Handles Snap-through. *Computers & Structures*, Volume 13(1-3), pp. 55–62

Dias, C.M.R., Savastano, Jr.H., John, V.M., 2010. Exploring the Potential of Functionally Graded Materials Concept for the Development of Fiber Cement. *Construction and Building Materials*, Volume 24(2), pp. 140–146

FIB Bulletin Nr. 55 and 56, 2010. *Model Code 2010, First Complete Draft*, Volume 1 and 2, ISBN 978-2-88394-095-3/6, Federal Institute of Technology, Lausanne, Switzerland

Gan, B.S., Aylie, H., Pratama, M.M.A., 2015. The Behavior of Graded Concrete, an Experimental Study. *Procedia Engineering*, Volume 125, pp. 885–891

Hidayat, A., Purwanto, Puspowadojo, J., Aziz, F.A., 2015. The Influence of Graded Concrete Strength on Concrete Element. *Procedia Engineering*, Volume 125, pp. 1023–1029

Hutton, D.V., 2004. *Fundamentals of Finite Element Analysis*, 1st edition, New York: McGraw-Hill

Kieback, B., Neubrand, A., Riedel, H., 2003. Processing Techniques for Functionally Graded Materials. *Materials Science and Engineering: A*, Volume 362(1-2), pp. 81–106

Mastali, M., Mastali, M., Abdollahnejad, Z., Ghasemi Naghibdehi, M., Sharbatdar, M.K., 2014. Numerical Evaluations of Functionally Graded RC Slabs. *Chinese Journal of Engineering*, Volume 2014, pp. 1–20

Pratama, M.M.A., 2015. An Experimental Finite Element Approach to the Behavior of Graded Concrete. *Master's Thesis*, Magister of Civil Engineering, Diponegoro University, Indonesia [in Bahasa]

Ramadhansyah, P.J., Abu Bakar, B.H., Megat Azmi, M.J., Wan Ibrahim, M.H., 2011. Engineering Properties of Normal Concrete Grade 40 Containing Rice Husk Ash at Different Grinding Times. *International Journal of Technology*, Volume 2(1), pp. 10–19

Ramu, I., Mohanty, S.C., 2014. Modal Analysis of Functionally Graded Material Plates using Finite Element Method. *Procedia Materials Science*, Volume 6, pp. 460–467

Shen, B., Hubler, M., Paulino, G.H., Struble, L.J., 2008. Functionally-graded Fiber-reinforced Cement Composite: Processing, Microstructure, and Properties. *Cement Concrete and Composites*, Volume 30(8), pp. 663–673

Shin, S.K., Kim, J.J.H., Lim, Y.M., 2007. Investigation of the Strengthening Effect of DFRCC Applied to Plain Concrete Beams. *Cement and Concrete Composites*, Volume 29(6), pp. 465–473

Banks-Sills, L., Eliasi, R., Berlin, Y., 2002. Modeling of Functionally Graded Materials in Dynamic Analysis. *Composites Part B: Engineering*, Volume 33(1), pp. 7–15

Stroeven, P., Hu, J., 2007. Gradient Structures in Cementitious Materials. *Cement Concrete and Composites*, Volume 29(4), pp. 313–323